Protein Expression Profiling of the *Drosophila* Fragile X Mutant Brain Reveals Up-regulation of Monoamine Synthesis*

Yong Q. Zhang‡§, David B. Friedman¶, Zhe Wang‖, Elvin Woodruff III‡, Luyuan Pan‡, Janis O'Donnell‖, and Kendal Broadie‡

Fragile X syndrome is the most common form of inherited mental retardation, associated with both cognitive and behavioral anomalies. The disease is caused by silencing of the fragile X mental retardation 1 (*fmr1*) gene, which encodes the mRNA-binding, translational regulator FMRP. Previously we established a disease model through mutation of *Drosophila fmr1* (*dfmr1*) and showed that loss of dFMRP causes defects in neuronal structure, function, and behavioral output similar to the human disease state. To uncover molecular targets of dFMRP in the brain, we use here a proteomic approach involving two-dimensional difference gel electrophoresis analyses followed by mass spectrometry identification of proteins with significantly altered expression in *dfmr1* null mutants. We then focus on two misregulated enzymes, phenylalanine hydroxylase (Henna) and GTP cyclohydrolase (Punch), both of which mediate in concert the synthetic pathways of two key monoamine neuromodulators, dopamine and serotonin. Brain enzymatic assays show a nearly 2-fold elevation of Punch activity in *dfmr1* null mutants. Consistently brain neurochemical assays show that both dopamine and serotonin are significantly increased in *dfmr1* null mutants. At a cellular level, *dfmr1* null mutant neurons display a highly significant elevation of the dense core vesicles that package these monoamine neuromodulators for secretion. Taken together, these data indicate that dFMRP normally down-regulates the monoamine pathway, which is consequently up-regulated in the mutant condition. Elevated brain levels of dopamine and serotonin provide a plausible mechanistic explanation for aspects of cognitive and behavioral deficits in human patients. *Molecular & Cellular Proteomics 4:278–290, 2005.*

Fragile X syndrome (FraX)[1] is a common form of inherited mental retardation manifesting a range of behavioral symptoms including cognitive defects, hyperactivity, hyperarousal, hypersensitivity to sensory stimuli, and impaired motor coordination (1, 2). FraX is caused by silencing of the fragile X mental retardation (*fmr1*) gene, which encodes an RNA-binding, translational regulatory protein (FMRP). FMRP associates with two structurally and functionally homologous proteins, fragile X-related 1 (FXR1P) and 2 (FXR2P) as well as several other proteins and RNAs in a complex that interacts directly with polyribosomes (for recent reviews, see Refs. 2–4). Several genomic and *in vitro* biochemical binding studies have delineated subsets of mRNA species that are bound to the FMRP complex (5–8). Although FMRP function may include the subcellular transport and/or stabilization of bound mRNAs, its best established function is to regulate, in most cases negatively, the translation of bound mRNAs (2, 9, 10). The challenge is to determine which FMRP mRNA targets are most critical for its *in vivo* functions and which FMRP-dependent interactions are altered when FMRP is absent to cause the most damaging FraX symptoms.

A mouse FraX model established in 1994 has provided the foundation for our current understanding of FMRP function (11). However, neuronal and behavioral phenotypes of *fmr1* knock-out mice appear relatively subtle and particularly sensitive to genetic background (12, 13). Moreover the genomic and *in vitro* biochemical binding studies of FMRP in mammals have generated a dauntingly long list of putative mRNA partners, increasing the difficulty of pinpointing the most relevant impacted pathways. Therefore, to complement the mouse model, a *Drosophila* FraX model was established in 2001 (14) to provide evolutionary perspective on conserved FMRP functions and to allow genetic studies of molecular and cellular functions in the context of a relatively simple brain (14–19). The *Drosophila* fragile X mental retardation (*dfmr1*) gene is the only family member present in the fly genome. FMRP and

From the ‡Department of Biological Science, Kennedy Center for Research on Human Development and the ¶Proteomics and Mass Spectrometry Research Center, Vanderbilt University, Nashville, Tennessee 37232-1634 and the ‖Department of Biological Sciences, University of Alabama, Tuscaloosa, Alabama 35487-0344

Received, November 8, 2004, and in revised form, December 20, 2004

Published, MCP Papers in Press, January 4, 2005, DOI 10.1074/mcp.M400174-MCP200

[1] The abbreviations used are: FraX, fragile X syndrome; 2D, two-dimensional; DIGE, difference gel electrophoresis; BH4, tetrahydrobiopterin; DA, dopamine; DCV, dense core vesicle; *dfmr1*, *Drosophila* fragile X mental retardation 1 gene; dFMRP, *Drosophila* fragile X mental retardation protein; *fmr1*, fragile X mental retardation 1 gene; FMRP, fragile X retardation mental retardation protein; FXR, fragile X-related; Henna, *Drosophila* phenylalanine hydroxylase; PTM, post-translational modification; Punch, *Drosophila* GTP cyclohydrolase; TH, tyrosine hydroxylase; CHAPS, 3-[(3-cholamidopropyl)dimethylammonio]-1-propanesulfonic acid.

dFMRP have in common all defined functional domains, post-translational modifications, subcellular expression pattern, and, where they have been assayed, RNA binding properties, interacting protein and RNA partners, and a conserved role as a translational repressor (2, 14–16, 20–22). In *Drosophila*, loss of dFMRP causes significant changes in neuronal structural morphogenesis and circuit formation (18, 19) and synaptic differentiation and neurotransmission properties (14, 19) and alterations in behavioral output (14–16) comparable to the human disease. To establish molecular bases for these cellular and behavioral phenotypes, it is particularly important to identify proteins that are misregulated in the absence of dFMRP.

To reveal dFMRP targets, we took a proteomic approach in the brain using two-dimensional difference gel electrophoresis (2D DIGE) followed by mass spectrometry and data base interrogation to identify proteins whose expression profiles are significantly altered in *dfmr1* null mutants. A surprisingly small set of proteins showed altered expression: 24 species that can be placed into five functional groups. The largest group (six proteins), containing the most dramatic changes in protein abundance, functions in energy metabolism. The second most impacted group contains two enzymes, phenylalanine hydroxylase (Henna) and GTP cyclohydrolase I (Punch), involved in biogenic amine synthesis. The other groups include heat shock proteins and protein degradation proteins (five proteins), cytoskeletal proteins (tubulin, actin, and tropomyosin), redox and ion homeostasis proteins (two proteins), and a collection of six miscellaneous proteins of no clear group or relationship to known aspects of dFMRP function. Since energy metabolism is relatively refractory to analyses of nervous system specific functions, we first focused our attention on the second most impacted group, proteins involved in the centrally important monoamine neuromodulator pathway.

Dopamine and serotonin are major neuromodulators in the central brain, mediating a wide range of cognitive functions and behavioral regulation in both vertebrates and invertebrates (23–26). In *Drosophila*, GTP cyclohydrolase is encoded by the *punch* gene. Punch protein converts GTP to dihydroneopterin triphosphate, the rate-limiting step in *de novo* synthesis of tetrahydrobiopterin (BH4), an essential cofactor for three aromatic amino acid monooxygenases, *i.e.* phenylalanine, tyrosine, and tryptophan hydroxylases, participating in the dopamine and serotonin syntheses (27, 28). In *Drosophila*, phenylalanine hydroxylases and tryptophan hydroxylase are encoded by a single gene, *henna* (29). Henna converts precursors phenylalanine and tryptophan into dopamine and serotonin, respectively, for the synthesis of serotonin. Henna is the rate-limiting enzyme (29). Thus, Henna and Punch, working in concert and in different steps, regulate the synthetic pathways of dopamine and serotonin. 2D DIGE reveals specific defects in the post-translational modification (PTM) of Henna and Punch in *dfmr1* mutant brains. The activities of both enzymes are positively regulated by PTM, *i.e.* phosphorylation (30–34). Consistently brain enzymatic assays reveal significantly increased activity of Punch in *dfmr1* mutants. Furthermore brain neurochemical assays show that various intermediates of the biogenic amine pathways are significantly increased in *dfmr1* mutants, including both dopamine and serotonin, consistent with proteomic and enzymatic assay results. Finally ultrastructural studies show a significant elevation in the number of dense core vesicles in synaptic terminals of *dfmr1* mutant brains. This class of secretory vesicle mediates release of neuromodulators including dopamine and serotonin. Taken together, these diverse data reveal up-regulation of the monoamine pathway in *dfmr1* mutant brains, suggesting a likely molecular mechanism for aspects of cognitive and behavioral deficits in human FraX patients.

EXPERIMENTAL PROCEDURES

Drosophila Stocks and Husbandry—The control genotype used in all experiments was w^{1118}; *FRT82B*. The *dfmr1* null mutant stock used in all experiments was w^{1118}; *FRT82B*, $dfmr1^{50M}$. This null allele of *dfmr1* is a small intragenic deficiency produced by imprecise P-element excision (14); it is completely viable, produces no detectable protein by immunocytochemistry staining or Western analyses, and is phenotypically indistinguishable from other characterized null mutant alleles (14, 16, 19, 35), one of which is completely rescued by a transgenic wild-type *dfmr1* gene (15). All *Drosophila* stocks were maintained at 25 °C on standard medium.

Proteomic Analysis—2D DIGE using a mixed sample internal standard, spot identification by mass spectrometry, and data base searching was done largely according to previous reports (35, 36). For each of three independent replicate experiments, 50 heads from 2-day-old adult flies (half male and half female) of each genotype (genetic control: w^{1118}; *FRT82B*; and mutant animal: w^{1118}; *FRT82B*, $dfmr^{50M}$) were homogenized in 100 μl of lysis buffer (7 M urea, 2 M thiourea, 4% CHAPS, 17 mM DTT), precipitated with methanol/chloroform, and resuspended in 100 μl of lysis/labeling buffer (7 M urea, 2 M thiourea, 4% CHAPS, 30 mM Tris, 5 mM magnesium acetate) prior to labeling with 200 pmol of either Cy3 (control) or Cy5 (mutant). In a similar fashion, 150 brains, 25 from each of the six samples (three controls and three mutants), were processed and labeled with 600 pmol of Cy2 (6-mix) as internal control for the three different gels. The labeled samples were combined such that each pair of Cy3- and Cy5-labeled samples was mixed with an equal aliquot of the Cy2-labeled mixed sample; in total, 150 brains (50 brains of each of labeled samples of control, mutants, and 6-mix) were loaded on the gel. The three sets of tripartite-labeled samples were separated by standard 2D gel electrophoresis using an IPGphor first dimension isoelectric focusing unit and 24-cm pH 4–7 immobilized pH gradient (IPG) strips (Amersham Biosciences) followed by second dimension 12% SDS-PAGE using an Ettan DALT 12 unit (Amersham Biosciences) according to the manufacturer's protocols. The Cy2 (mixed standard), Cy3 (control), and Cy5 (mutant) components of each gel were individually imaged using mutually exclusive excitation/emission wavelengths of 480/530 nm for Cy2, 520/590 nm for Cy3, and 620/680 nm for Cy5 with a 2D 2920 Master Imager (Amersham Biosciences). A Sypro Ruby poststain (Molecular Probes) was used to ensure accurate protein excision as the low stoichiometry of CyDyes label only 1–3% of the total protein. DeCyder software (Amersham Biosciences) was used for simultaneous comparison of abundance changes across all three sample pairs with statistical confidence and without interference from gel-to-gel variation (36, 37). Control:mutant volume ratios for each protein were calculated relative to the internal

standard present on every gel and were used to calculate average abundance changes and Student's *t* test probability (*p*) values for the variance of these ratios for each protein pair across all three independent gels. Entries with abundance changes of ≥1.3-fold increase or decrease, an arbitrary cut-off, and *p* values ≤0.05 are reported. Proteins of interest were excised and digested in-gel with modified porcine trypsin protease (Promega). MALDI-TOF mass spectrometry was performed on a Voyager 4700 (Applied Biosystems). Ions specific for each sample were used to interrogate *Drosophila* sequences deposited in the Swiss-Prot and National Center for Biotechnology Information (NCBI) data bases using the MASCOT (www.matrixscience.com) and ProFound (prowl.rockefeller.edu) search algorithms, respectively.

Enzymatic Activity Assay—Punch enzymatic activity was assayed largely according to previous reports with the reaction product quantified by HPLC (38, 39). Fly heads from 24-h posteclosion adults were collected by sieving from liquid N_2-frozen and vortexed flies. Fifty heads were homogenized in 100 μl of cold 50 mM Tris, pH 8.0, containing 2.5 mM EDTA, 5% sucrose, and Roche Applied Science protease inhibitor mixture. After centrifugation of the homogenates at 9300 × *g* for 10 min at 4 °C, 5 mg of acid-rinsed charcoal was added to 100 μl of supernatant with gentle mixing to adsorb eye pigment. After centrifugation to remove the charcoal, the protein concentration of the extract was determined using a Bio-Rad protein assay kit. Extract (45 μg of protein/ml) was mixed with GTP to a substrate concentration of 2 mM in a final volume of 70 μl. The reaction was incubated at 37 °C for 1 h after which the product of the reaction, 7,8-dihydroneopterin triphosphate, was oxidized to its fluorescent form in 30 μl of 1% iodine and 2% potassium iodide in 1 M HCl. After incubation of the oxidation solution for 1 h in the dark at room temperature, the samples were centrifuged at 14,500 × *g* for 5 min. The oxidation reaction was terminated, and the samples were decolorized with the addition of 15 μl of 3% ascorbic acid. After adjusting the samples to pH 8.0, 50 μl of each sample was mixed with 2 μl of calf intestine alkaline phosphatase, 7 μl of alkaline phosphatase buffer (Roche Applied Science), and 11 μl of distilled H_2O. The mixtures were incubated at 37 °C for 30 min to dephosphorylate the neopterin triphosphate product. The reaction mixture was centrifuged, and the supernatant was filtered. Reaction products (10 μl) were separated by HPLC on an ESA CoulArray system with Model 582 pumps using a Waters Symmetry C_{18} HPLC column (4.6 × 150 mm, 5-μm particle size). Pteridines were detected by fluorescence using an ESA Model LC305 fluorescence detector at excitation 360 nm/emission 456 nm. The specific activities were determined by integration of the peak area of neopterin, which appeared around 3 min using commercial neopterin (Sigma) as a standard. The specific activity of Punch is reported as nanomoles of neopterin generated per milligram of protein per minute of reaction time. The means and standard deviations of three independent activity assays were compared and analyzed by Student's *t* test using the SPSS statistics program.

Biogenic Amine Assay by HPLC—HPLC assays of biogenic amines and amino acids were done largely according to previous reports (40–42). Briefly 20 fly heads from 2-day-old flies (half male and half female) were homogenized in 150 μl of 0.1 M TCA, which contained 10 mM sodium acetate, 0.1 mM EDTA, 1 μM isoproterenol (as internal standard), and 10.5% methanol (pH 3.8). Samples were then centrifuged in a microcentrifuge at 10,000 × *g* for 20 min. The supernatant was removed and stored at −80 °C degrees. Before injection into the HPLC system, the supernatant was thawed and centrifuged again for 20 min. The HPLC system for biogenic amine measurement consisted of a Waters Model 515 pump, Waters 717+ autosampler, and an Antec electrochemical detector utilizing an Antec Decade (oxidation, 0.7) electrochemical detector. 20-μl samples of the supernatant were injected using a Water 717+ autosampler onto a Waters Nova-Pak C_{18} HPLC column (3.9 × 300 mm). Biogenic amines were eluted with a mobile phase consisting of 89.5% 0.1 M TCA, 10 mM sodium acetate, 01 mM EDTA, and 10.5% methanol (pH 3.8). Solvent was delivered at 0.7 ml/min using a Waters 515 HPLC pump. Using this HPLC solvent the four biogenic amines from fly heads elute in the following order: octopamine, dopamine, tyramine, and serotonin (42). Amino acids were determined by the Waters AccQ-Tag system utilizing a Waters 474 scanning fluorescence detector. 10-μl samples of the supernatant were diluted with 70 μl of borate buffer to which 20-μl aliquots of 6-aminoquinol-*N*-hydroxysuccinimidyl carbamate were added to form the fluorescent derivatives. After incubating the mixture for 10 min at 37 °C, 10 μl of resultant samples were injected into the HPLC system consisting of a Waters 712 autosampler, two 510 HPLC pumps, a column heater (37 °C), and a fluorescence detector. Separation of the amino acids was accomplished by means of a Waters amino acid column and supplied buffers (buffer A: 19% sodium acetate, 7% phosphoric acid, 2% triethylamine, 72% water; buffer B: 60% acetonitrile) using a specific gradient profile. Using this HPLC solvent system, the amino acids elute in the following order: cysteine, homocysteine, aspartic acid, serine, glutamate, glycine, taurine, arginine, threonine, alanine, proline, γ-aminobutyric acid, cystine, tyrosine, valine, methionine, lysine, isoleucine, leucine, and phenylalanine (40). HPLC control and data acquisition were managed by Millennium 32 software. The means and standard deviations of at least 17 repeats were analyzed using Student's *t* tests.

Brain Immunocytochemistry—Immunostaining of the adult brain was done largely according to previous reports (14, 19). Briefly brains from 2–3-day-old animals were dissected out intact in PBS followed by fixation in 4% formaldehyde for 30–45 min. For immunostaining, a rabbit polyclonal antibody against tryosine hydroxylase (Chemicon International) was used at a 1:300 dilution to visualize dopaminergic neurons. Mouse monoclonal antibody 22A7 against dFMRP was used at a 1:1000 dilution (20). Serial sections of antibody-stained brains were acquired on a Zeiss LSM 510 Meta laser scanning confocal microscope. Images were processed and presented with Adobe Photoshop 7.0.

Brain Electron Microscopy—Transmission electron microscopy ultrastructural analyses of *Drosophila* brains were done largely according to a previous report (19). Briefly 1–3-day-old adult brains for control and *dfmr1* mutants were dissected in PBS buffer and immediately fixed for 1 h in 2% glutaraldehyde at 4 °C. Samples were washed in PBS and transferred to 1% osmium tetroxide in double distilled H_2O for 1 h and stained *en bloc* in 2% aqueous uranyl acetate for 1 h. Samples were then dehydrated and embedded in araldite. After placing in a vacuum oven for 30 min, brains were placed in fresh araldite and left to polymerize overnight in a 60 °C oven. Ribbons of thin (~50-nm) sections were obtained with a Leica Ultracut UCT 54 ultramicrotome and examined on a Phillips CM12 transmission electron microscope. Digital electron microscopy images were taken of defined synaptic boutons from regions in the central brain. All sections for quantification contained at least one clear presynaptic T-bar active zone defining a release site (43). Dense core vesicles (DCVs) containing neuromodulators were counted in each synaptic profile. Over 50 synaptic profiles across the central brain were quantified. Statistical significance was determined by Student's *t* test.

RESULTS

Protein Expression Profiles Altered in dfmr1 Null Mutant Brains—FMRP/dFMRP is an mRNA-binding protein that associates with both polyribosomes and RNA interference/micro-RNA machinery to act as a translational regulator (5, 44–47). Studies in mouse and human suggest that FMRP

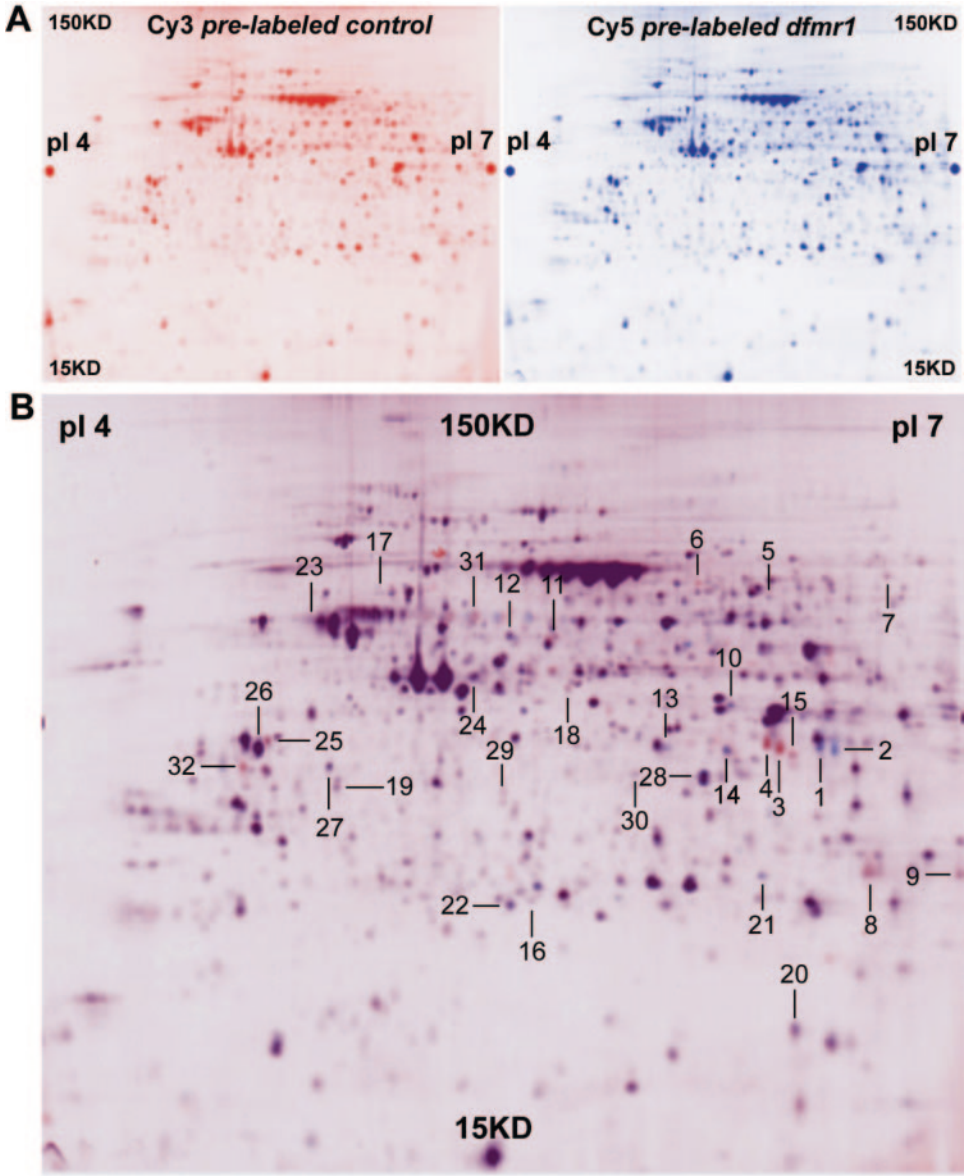

FIG. 1. **Proteomic analysis of *dfmr1* mutant brain.** *A*, representative 2D gels of brain protein samples. Control is labeled with Cy3 (*left*, *red*), and *dfmr1* null mutant is labeled with Cy5 (*right*, *blue*). The protein size range from 15 to 150 kDa (*bottom* to *top*) and pI range from 4 to 7 (*left* to *right*) are indicated. The expression profiles of the two brains look highly similar. *B*, the merged gel of wild-type and mutant protein samples. Protein spots with significantly altered expression profiles are *numbered*. Proteins with dramatically increased expression (>3-fold) in the mutants are seen as *blue spots* (*e.g. spots 1* and *2*). Proteins with dramatically decreased expression (>3-fold) in the mutants are seen as *red spots* (*e.g. spots 3* and *4*). Quantitative measurements are made relative to a Cy2-labeled internal standard co-migrating within the gel (not shown).

binds a large assortment of hundreds of putative target messages (*i.e.* 432 mRNAs in the mouse) (5, 7), but, as yet, only a few proteins (<5 total, *e.g.* microtubule-associated protein 1B and glucocorticoid receptor α) have been shown to display detectably altered expression *in vivo* in the absence of FMRP (7, 10). Thus, the scope of the role of FMRP as a translational regulator *in vivo* is entirely unclear. Using the *Drosophila* model, we wished to systematically analyze protein expression profiles in the *dfmr1* null mutant brain to identify candidate proteins to mechanistically associate with mutant phenotypes in neuronal structural elaboration, synapse differentiation, and the execution of complex behaviors (2, 14, 19). We therefore took advantage of a recently developed proteomic 2D DIGE approach (see "Experimental Procedures") to compare protein expression profiles in *dfmr1* null mutant brains relative to matched genetic controls (Fig. 1).

The 2D DIGE approach resolved ~1500 protein species in the brain. On first comparison, the protein expression profiles in mutant and control were strikingly similar, and it was apparent that there is no dramatic or widespread alteration in

TABLE I
Altered protein expression in dfmr1 mutant brain

Protein	Gel ID	Change[a]
Energy metabolism		
Glycerol-3-phosphate dehydrogenase	1	+4.53[b]
	2	+7.09[b]
	3	−4.41[b]
	4	−3.10[b]
Glucose-phosphate dehydrogenase	5	−1.3[c]
Electron-transferring flavoprotein	6	−3.49[d]
PckA phosphoenolpyruvate carboxykinase	7	−1.54[c]
Alcohol dehydrogenase	8	−1.66[d]
	9	−1.36[d]
Pyruvate dehydrogenase (CG7010)	10	+1.36[d]
Monoamine pathway		
Phenylalanine hydroxylase (Henna)	11	−1.68[d]
	12	+1.63[d]
GTP cyclohydrolase (Punch)	13	+2.43[c]
	14	+2.09[d]
	15	−2.52[c]
Hsp and protein degradation		
Heat shock protein 23	16	+1.42[c]
Heat shock protein 60	17	+1.61[d]
Cathepsin K (CG4847)	18	−1.4[d]
Cysteine proteinase 1	19	+1.52[d]
Ubiquitin-like 4 (CG7217)	20	+2.53[b]
Redox and ion homoestasis		
1-cys peroxiredoxin	21	+2.08[c]
Ferritin 1 heavy chain homolog	22	+1.66[c]
Cytoskeleton proteins		
β-tubulin	23	+1.31[d]
Actin 5C	24	+1.3[c]
Tropomyosin	25	−1.48[b]
	26	+1.38[c]
Miscellaneous		
Annexin IX	27	+1.51[c]
Senescence marker protein (SMP-30)	28	+2.33[b]
Spermine synthetase homolog (CG8327)	29	−1.42[d]
CG10997	30	+1.38[d]
Crystallin (CG16963)	31	−1.51[d]
Farnesoic acid methyltransferase (CG10527)	32	−2.45[b]

[a] +, increased expression; −, decreased expression.
[b] $p < 0.001$.
[c] $0.001 < p < 0.01$.
[d] $0.01 < p < 0.05$.

protein expression in the *dfmr1* null mutant brain (Fig. 1*A*) in contrast to predictions (5, 7). Protein abundance for each species was quantified and compared using the DeCyder software to ensure that abundance changes across all sample pairs were calculated with statistical confidence and without interference from gel-to-gel variation (37). This approach indicated that <2% (24 of 1500) of detectable proteins were significantly altered in *dfmr1* null mutant brains compared with controls; only 24 proteins change expression level by ≥1.3-fold (increase or decrease) (Fig. 1*B* and Table I). Moreover these 24 proteins can be assigned into just five functional categories plus a small group of unrelated proteins. The largest group (six proteins), containing the largest -fold changes in protein abundance, functions in energy metabolism, including glycerol-3-phosphate dehydrogenase and glucose-phosphate dehydrogenase (Table I). These changes are consistent with alteration in glucose metabolism in *fmr1* knock-out mice (48). The second largest group (five proteins) functions as heat shock protein chaperones and other proteins involved in protein maintenance *versus* degradation pathways (Table I). The up-regulation of these proteins likely reflects conditions of increased metabolic and/or general cellular stress (49). The third group (three proteins) is cytoskeletal proteins (β-tubulin, actin, and tropomyosin). The identification of these proteins are consistent with a number of earlier reports predicting alteration in both actin and microtubule cytoskeletal dynamics and stability (9, 14, 50). The fourth group encodes two components of the monoamine biosynthesis pathway, suggesting an alteration in neuromodulator production, consistent with recent mammalian reports (51). This group will be our primary focus in this study (see below). The last two groups include two proteins linked to redox changes/ion homeostasis and a collection of six miscellaneous proteins (Table I). These proteins belong to no clear functional group and have no relationship to known aspects of dFMRP function, and their significance is currently unknown.

Many of the protein expression changes in the *dfmr1* mutant brain suggest that the alterations are not due to direct dFMRP translation regulation but rather represent indirect interactions attributable to altered post-translational modification (Fig. 1*B* and Table I). In the energy metabolism group, for example, the most strongly impacted protein, glycerol-phosphate dehydrogenase, is altered in four different PTM isoforms (Table I); two isoforms are increased in abundance (7- and 4.5-fold), and two are decreased in abundance (4.4- and 3-fold). Four other proteins, alcohol dehydrogenase, Henna, Punch, and tropomyosin, also show two or more isoforms with altered expression profiles (Table I). These proteins with multiple isoforms changing in opposite directions again suggest indirect post-translational modification defects in *dfmr1* mutants. The mechanism of these modifications is unknown as our screen did not identify any kinase, phosphatase, or other protein class known to mediate these post-translational modification events. It is intriguing to note, however, there are several kinases and phosphatases whose mRNAs are reportedly direct targets of FMRP binding (7).

The Monoamine Synthesis Pathway Is Activated in the dfmr1 Mutant Brain—The two enzymes Henna and Punch participate in the same synthetic pathway for biogenic amines dopamine and serotonin, suggesting that regulation of this biosynthetic neuromodulator pathway could be a significant target of dFMRP regulation. The mass spectra of gel-excised proteins identified multiple isoforms of both Punch and Henna to be significantly misregulated in the *dfrm1* null mutant brain (Fig. 2). MALDI-TOF fragmentation spectra confirmed the post-translationally modified isoforms of the enzymes. Magnified comparison of control and mutant 2D DIGE gels showed changes in three Punch PTM isoforms, which was

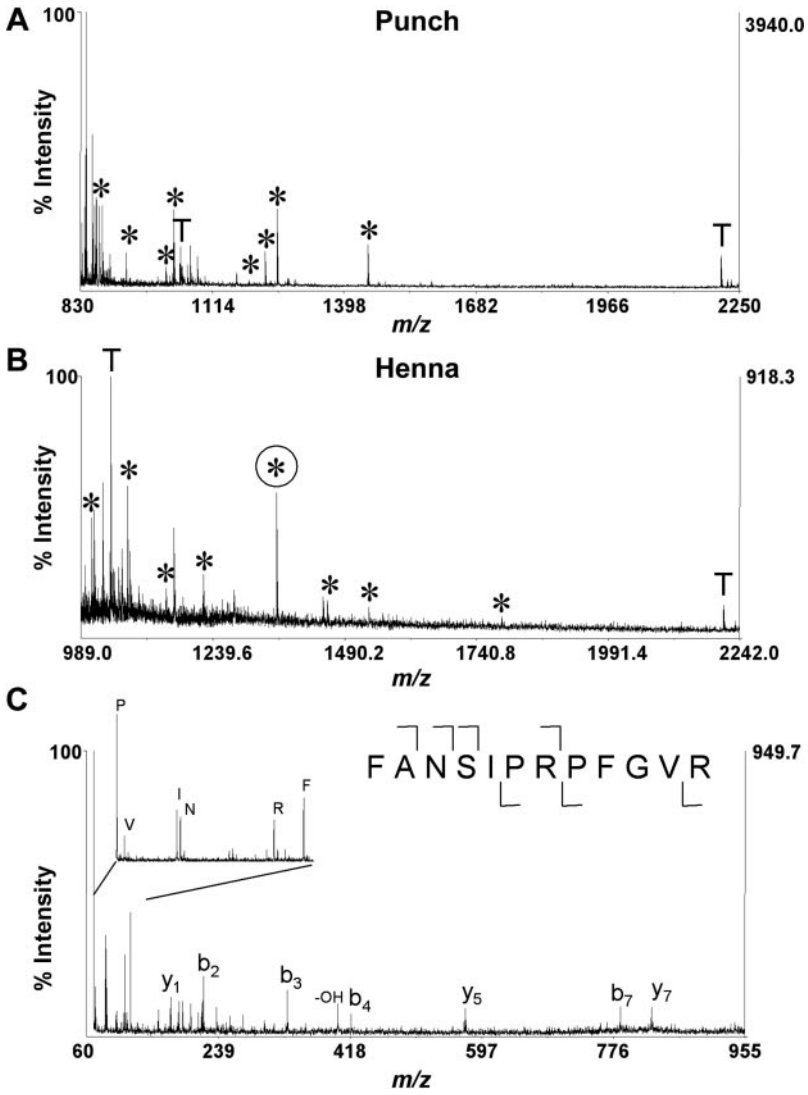

FIG. 2. **Identification of protein by mass spectrometry.** *A*, mass spectra of gel-excised proteins used for protein identification. MALDI-TOF peptide mass maps of one of the isoforms of Punch (*A*) and Henna (*B*). Trypsin autolytic peptides indicated by *T* are used to internally calibrate spectra to accuracy within 20 ppm. *Asterisks* denote peptide ion masses matching the predicted protein with statistical confidence within the 95th percentile using either MASCOT (MOWSE = 66 (49) and 126 (57), respectively) or ProFound (z-score = 1.92 and 2.39, respectively; values >1.65 within 95th percentile) algorithms. *C*, MALDI-TOF/TOF fragmentation spectrum for *m/z* (*x axis*) 1360.91 ion (*circled* in *B*) from the acidic Henna isoform. y- and b-ion and immonium ions (on the *expanded axis*) are denoted, and cleavages are summarized on the sequence (b-ions *above*; y-ions *below*). The *m/z* 1360.91 ion (*circled* in *B*) was the only ion from the acidic Henna isoform requiring this confirmation by tandem mass spectrometry. The peptide mass maps for Punch were sufficient for identification without further analyses by tandem mass spectrometry.

consistent across all three replicates (Fig. 3*A*, compare with Fig. 1*B* (*spots 13–15*) and Table I (spots 13–15)). The abundance levels from each PTM isoform can also be represented as a three-dimensional pixel intensity map of the control *versus* the mutant species (Fig. 3*B*) or graphical representation of the average protein abundance change across all trials (Fig. 3*C*). The average protein abundance change for the three PTM isoforms, from the most acidic isoform to the most basic isoform, was a 2.43-fold increase ($p = 0.001$), 2.09-fold increase ($p = 0.01$), and 2.52-fold decrease ($p = 0.008$). Similar changes occur to Henna with two PTM isoforms changing in opposite directions (Fig. 1*B* (*spots 11* and *12*) and Table I (spots 11 and 12)). Taken together, these data indicate a highly significant shift in the abundance of the PTM isoforms of these enzymes in the *dfmr1* mutant brain.

Henna and Punch are involved in the same biogenic amine synthesis pathways (Fig. 4*A*). Punch is the rate-limiting enzyme in the synthesis of BH4, an essential cofactor for the activity of Henna and the other two aromatic amino acid monooxygenases tyrosine and tryptophan hydroxylases (28). In Fig. 4*A*, the three *asterisks* indicate the three steps in the synthetic pathway of biogenic amines dopamine and serotonin that require BH4. In *Drosophila*, Henna and tryptophan hydrogenase are encoded by the same gene (29). To determine the functional consequences of the PTM isoform protein expression changes revealed in the proteomic analyses, the enzymatic activities of Punch from control and mutant brains were assayed using an established protocol (see "Experimental Procedures") (39). The activity of Punch is nearly doubled in the *dfmr1* null mutant brain from 0.14 nmol of neopterin/mg of protein/minute of reaction time in control to 0.24 in mutants (Fig. 4*B*; $p < 0.05$, $n = 3$). Mammalian studies have shown that Punch enzymatic activity is regulated by phosphorylation with the phosphorylated form of Punch having higher enzymatic activity (33). The increased enzymatic activity of Punch in *dfmr1* mutants is consistent with the proteomic results that the more acidic, probably phosphorylated Punch isoforms (*spots 13* and *14*) are increased, concomitant with a decrease

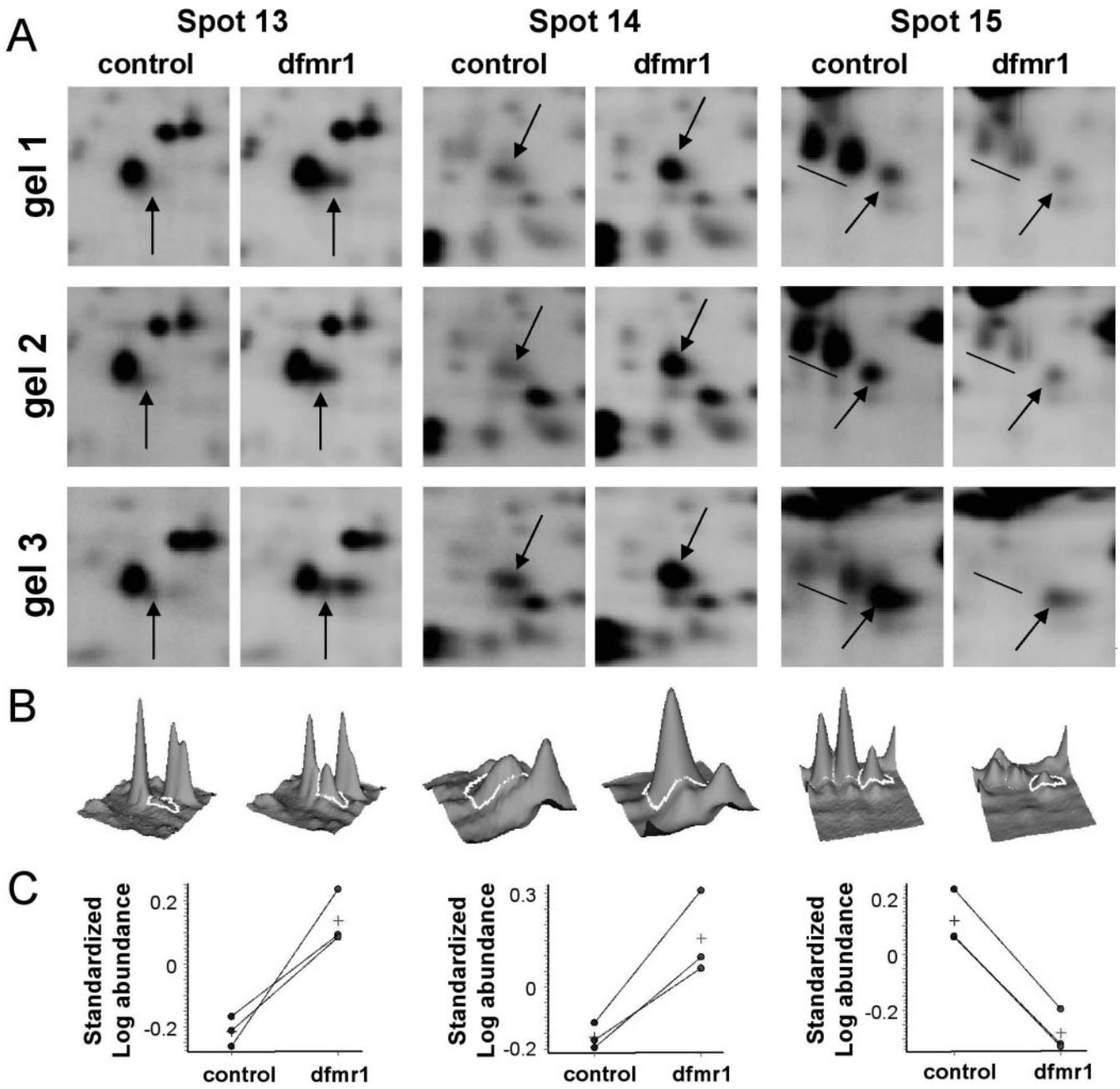

FIG. 3. **Changes in post-translational modification of three Punch isoforms**. *A*, separate Cy3-labeled control and Cy5-labeled mutant gel images are shown for each of three punch isoforms (*arrows*) in the three DIGE gels (corresponding to proteins *spots 13*, *14*, and *15* in Fig. 1 and Table I). Data for the most acidic isoform are presented in the *right-hand* pair of images, and the basic isoform is presented in the *left-hand* pair of images. Two isoforms of glycerol-3-phosphate dehydrogenase *underlined* in the *right-hand* pair of images are also changing in abundance. *B*, abundance levels from one of the three comparisons are shown for each isoform as a three-dimensional representation of the pixel intensity of the Cy3-labeled control *versus* Cy5-labeled mutant signal (*bounded in white*). *C*, graphical representation of the average abundance change indicated by *crosses* between control (*blue cross*) and *dfmr1* mutants (*red cross*). Measurements were made within each gel and normalized using the Cy2-labeled internal standard (standardized log abundance). Average relative abundance changes for the three isoforms, from acidic to basic, are as follows: 2.43-fold increase for *spot 13* ($p = 0.0017$), 2.09-fold increase for *spot 14* ($p = 0.016$), and 2.52-fold decrease for *spot 15* ($p = 0.0087$).

in the basic, probably dephosphorylated Punch isoform (*spot 15*). Interestingly Punch mRNA was also found to be a target directly regulated by mammalian FMRP (7).

The Levels of Dopamine and Serotonin Are Increased in dfmr1 Mutant Brain—The biogenic monoamine neuromodulators dopamine and serotonin play critical roles in the regu-

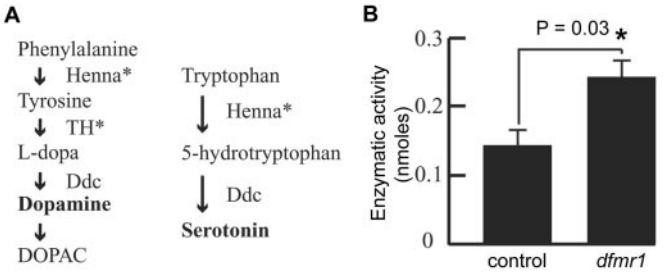

FIG. 4. **Punch enzymatic activity is elevated in *dfmr1* mutant brain.** *A*, biosynthetic pathway of neuromodulator monoamines dopamine and serotonin. *L-Dopa*, the levorotatory form of dihydroxyphenylalanine; *Ddc*, dihydroxyphenylalanine decarboxylase. Both Henna and Punch (*asterisk*) require BH4 as a cofactor. Punch is the rate-limiting enzyme required for BH4 synthesis and, thus, monoamine production. *B*, enzymatic activity of Punch is significantly increased ($p < 0.05$) in *dfmr1* null mutants compared with control. Activity is defined as nanomoles of neopterin per milligram of proteins per minute of reaction. *Error bars* show mean ± S.D.; $n = 3$.

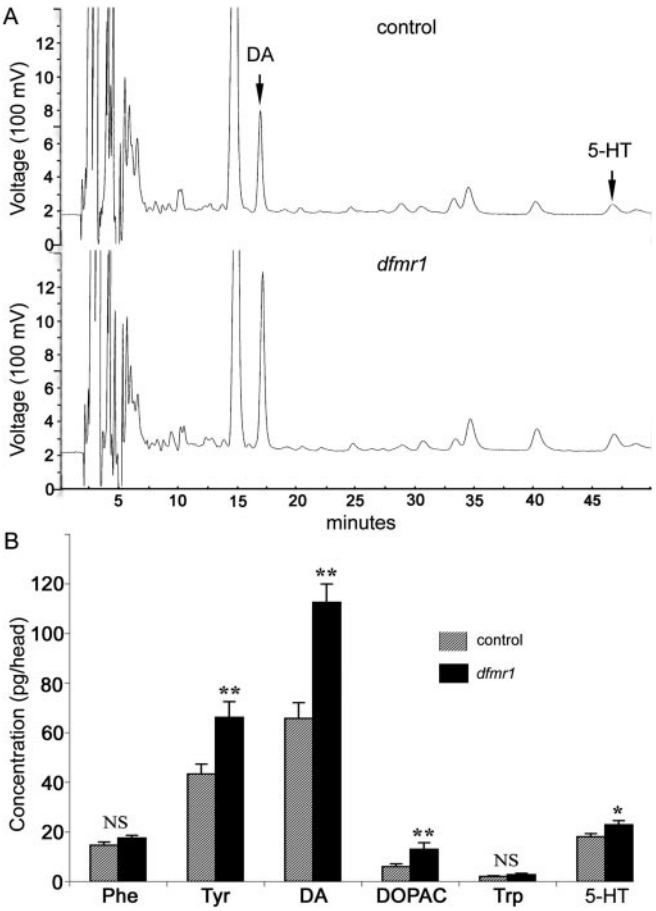

FIG. 5. **Dopamine production up-regulated in *dfmr1* mutant brain.** *A*, representative HPLC traces of biogenic amines from head extract from both control and *dfmr1* null mutants. The peaks of dopamine (*DA*) and serotonin (*5-HT*) are indicated. *B*, the concentrations of different metabolites in the monoamine synthetic pathway. Samples from control are shown in *hatched bars*; mutants are shown in *black bars*. *Error bars* indicate mean ± S.D. * indicates $0.05 > p > 0.01$; **, $p < 0.01$. $n \geq 18$; *NS*, not significant.

lation of complex behaviors, including motor control, activity level, and learning, in both vertebrates and invertebrates (23–26). These functions are particularly relevant to FraX, characterized by defects in motor control, activity level, and learning ability. The above proteomic analyses show that the monoamine synthesis pathway is under the control of dFMRP regulation at two levels, Henna and Punch. Specifically the PTM isoforms of both proteins are both significantly shifted to more acidic, probably phosphorylated states. Both Henna and Punch are activated by phosphorylation and inactivated when dephosphorylated (30–32). Consistently Punch enzymatic activity is elevated in the *dfmr1* null mutant brain (Fig. 4*B*), and the acidic isoform of Henna (Fig. 1*B*, *spot 11 versus spot 12*) is predicted to be similarly activated. Henna is the first enzyme in the synthesis cascade of both dopamine and serotonin (Fig. 4*A*). Tyrosine hydroxylase (TH) is the rate-limiting enzyme in the dopamine synthesis pathway downstream of Henna (52) (Fig. 4*A*). Both Henna and TH require the regulatory cofactor BH4 whose synthesis depends on Punch as the rate-limiting enzyme. Taken together, these results predict that the dopamine and serotonin biosynthetic pathway should be accelerated in the absence of dFMRP.

A neurochemistry approach utilizing HPLC was used to assay the abundance of dopamine and serotonin, and their precursors and products, in the *Drosophila* brain (see "Experimental Procedures"). HPLC assays were done of both amino acids and biogenic amines in age-matched genetic controls and *dfmr1* null mutants (Fig. 5*A*). In mutants, 13 of the 19 amino acids assayed remain unchanged, although serine, glutamate, histidine, alanine, γ-aminobutyric acid, and tyrosine show significant, mild increases ($p < 0.05$; data not shown). However, metabolites of the dopamine synthetic pathway downstream of the amino acid precursor phenylalanine through tyrosine to dopamine and finally to the dopamine product 3,4-dihydroxyphenylacetic acid are all significantly increased in mutants (Fig. 5*B*). In particular, the level of dopamine is elevated by 80% in mutants from 63 pg/head in control to 114 pg/head in *dfmr1* nulls, a highly significant increase ($p < 0.01$). A possible caveat to all of these analyses is that they were done on the entire head, and the cuticle is also known to contain dopamine at least during development. The turnover of dopamine, *i.e.* the 3,4-dihydroxyphenylacetic acid/dopamine ratio, remains unchanged between mutant and control. Serotonin is also significantly elevated in abundance but to a lesser extent (30% increase) from 17 pg/head in controls to 22 pg/head in *dfmr1* nulls, a significant increase ($p < 0.05$; Fig. 5*B*). Taken together, the different lines of evidence from proteomic, enzymatic, and neurochemical assays indicate that the biosynthesis pathways of dopamine and serotonin, and thus the levels of dopamine and serotonin, are up-regulated in *dfmr1* mutant brains by a mechanism in which dFMRP negatively regulates the activity of Henna and Punch via post-translational modification.

Dense Core Vesicles Are Increased in the dfmr1 Mutant Brains—The up-regulation of neuromodulators dopamine and serotonin in *dfmr1* mutants provides a plausible mechanistic explanation for behavioral defects observed in the *Drosophila* model and, by extension, in human FraX patients. Therefore, we wished to explore further the cellular and subcellular basis of this mechanism. One possibility is that *dfmr1* mutants might display more, or structurally overgrown, neurosecretory neurons within these modulatory pathways. To test this possibility, control and *dfmr1* mutant brains were stained with anti-TH to assay dopaminergic neurons. Double labeling with anti-dFMRP and anti-TH shows that dFMRP is highly expressed in dopaminergic neurons in the central brain (Fig. 6*A*), consistent with the role of dFMRP in regulating the dopamine biosynthesis pathway. However, no discernible morphological abnormalities were found in TH-producing dopaminergic neurons in *dfmr1* null mutants (data not shown). These data suggest that the normal complement of dopaminergic neurons must be overproducing dopamine in the mutant condition.

Electron microscopy analyses were used next to probe the ultrastructure of central brain synaptic connections, particularly to assay for alterations consistent with an up-regulation of the neurosecretory pathway. A subset of neurosecretory vesicles are enlarged and contain an electron-dense core due to the presence of electron-dense proteins within the vesicle lumen. These DCVs (Fig. 6*B*) specifically package neuromodulators including neuropeptides and biogenic amines such as dopamine and serotonin. Therefore, the distribution of DCVs was assayed in control and mutant brains. All quantification was done in identified synaptic profiles defined by the clear presence of a presynaptic electron-dense T-bar, which marks synaptic active zones (43). DCVs per synaptic profile were quantified in the central brain for both control and *dfmr1* null mutants. In mutant brains, the number of DCVs is significantly ($p = 0.008$) increased from 2.6 ± 0.6 DCVs/bouton in control to 6.4 ± 0.9 in mutants (Fig. 6, *B* and *C*). This ultrastructural finding strongly supports the conclusion that dopamine/serotonin pathways are aberrantly elevated in the *dfmr1* mutant brain and suggests that increased release of these neuromodulators may be an important element of the FraX disease condition.

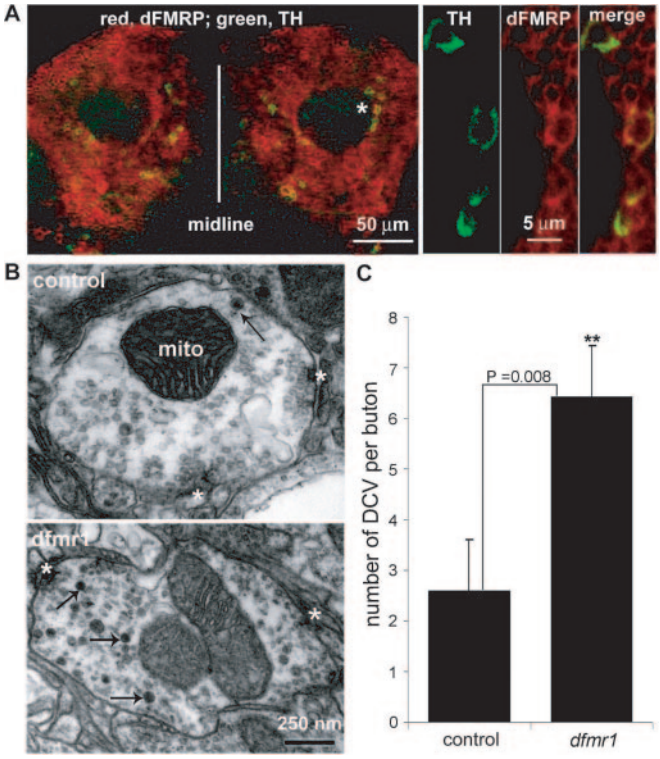

FIG. 6. **Increased number of dense core vesicles in *dfmr1* mutant brain.** *A*, dFMRP is expressed in dopaminergic neurons in the brain. An adult brain double labeled with anti-dFMRP (*red*) and anti-TH (*green*) to reveal dopaminergic neurons is shown. In the *left* image, a low magnification brain image is shown with the *asterisk* marking the synaptic neuropil with no staining of either antibody. A number of TH-positive neurons are shown in *green*. In the *right* images, higher magnification is shown of the co-localization of dFMRP and TH in single dopaminergic neurons. *B*, electron micrograph (40,000×) of single synaptic boutons from control and *dfmr1* mutant brains. Control bouton shows two active zones (*asterisks*), synaptic vesicles, and DCVs, one of which is marked by an *arrow*. In contrast, the *dfmr1* mutant (*bottom left panel*) has much more numerous DCVs, three marked by *arrows*. The *scale bar* represents 250 nm. *C*, quantification of DCV numbers in control and *dfmr1* mutant synaptic terminals. The *dfmr1* null mutant animals display a significantly increased number of DCVs ($p = 0.008$) throughout synaptic boutons in the brain of adult animals. *Error bars* show mean ± S.D. (control, $n = 21$; *dfmr1*, $n = 32$). **, $p < 0.01$. *mito*, mitochondria.

DISCUSSION

dFMRP-dependent Protein Changes in the Brain—RNA binding studies and microarray analysis have identified hundreds of potential direct mRNA targets of FMRP binding and translational regulation (5, 7). However, few proteins have been clearly demonstrated to be *in vivo* targets despite considerable effort. This discrepancy may reflect the fact that microarray analyses have overestimated the number of true FMRP targets or that these targets are regulated in highly specific temporal and/or spatial patterns that may be exceedingly difficult to verify *in vivo*. In this study, we have therefore taken the unique approach of searching for brain protein targets directly by using 2D DIGE coupled to mass spectrometry identification of proteins altered in abundance in *dfmr1* null mutants. This proteomic approach has the advantage that it directly identifies brain proteins whose abundance *in vivo* is dependent on dFMRP; it identifies not only direct targets of dFMRP regulation but also any proteins altered secondarily or as an indirect consequence of *dfmr1* mutant phenotypes. However, like all screening approaches, this proteomic analysis does not approach saturation. Among other things, this proteomic analysis is limited in the size and abundance of proteins it can detect by the temporal period of analysis and by the whole-brain nature of the experiment. Thus, we do not expect this approach to have identified large (>150 kDa) or

rare proteins, proteins altered only during a specific developmental window, or proteins altered only in a small region of the brain. Rather this proteomic approach reveals expression changes of relatively small, relatively abundant proteins in the adult brain. Future directions for overcoming the current proteomic limitations will include assays of different developmental periods and specific brain regions and using cellular fractionations to identify protein changes limited to certain cellular compartments such as synaptosomes.

Bearing these caveats in mind, it is nevertheless striking to note how few proteins are altered in abundance in the complete absence of dFMRP; among ~1500 brain proteins analyzed, only 24 were significantly changed. It is interesting to note that the amplitude of changes shown in *dfmr1* null mutant brains is generally mild and mostly within a 4-fold range (Table I) compared with dramatic changes of protein expression profiles reported in other conditions (up to 20-fold) (36, 53). These limited protein changes are consistent with the viable nature of the mutation, the selective disruption of only complex behaviors, and the relatively subtle neuronal phenotypes at cellular and subcellular levels (14, 19). Moreover several of the protein changes appear to reflect shifts in the balance of PTM isoforms, *i.e.* a shift from one isoform (decreased) to another (increased) in the absence of dFMRP. This observation suggests that these proteins are indirect targets of dFMRP, indicating that dFMRP affects PTM pathways. Although not recovered in this screen, there are several kinases and phosphatases that have been reported as direct targets of FMRP (7). It is therefore probable that dFMRP regulates PTM isoforms of downstream targets via phosphorylation and dephosphorylation signaling pathways.

What is the functional significance of the protein expression changes in the *dfmr1* null mutant brain? Compared with the hundreds of putative mRNA targets uncovered by genomic approaches (5, 7), the 24 proteins uncovered by this proteomic strategy represent a manageable number of candidates to ascertain possible interactions with dFMRP one by one. The largest changes, and the largest impacted group, are proteins involved in energy metabolism (Table I), suggesting an alteration of fundamental metabolic pathways. This discovery is consistent with the increased rates of glucose metabolism in *fmr1* knock-out mouse brains (48). The second largest group, heat shock protein chaperones and proteins involved in protein degradation, redox, and ion homeostasis (Table I), indicates that the central neurons are generally under stress when dFMRP is absent. This could be a simple consequence of the increased metabolic rate of the mutant brain. We therefore focused attention on the physiological and pathological significance of the other two groups of dFMRP-dependent proteins, cytoskeleton proteins and biogenic amine synthesis enzymes. We discuss these two groups below.

dFMRP Negatively Regulates Cytoskeleton Stability—Our previous work has shown that dFMRP plays a prominent role in regulating the stability of the microtubule cytoskeleton both during spermatogenesis in the testes (35) and during synaptogenesis in the nervous system (14). In neurons, dFMRP acts as a direct negative translational regulator of Futsch, the *Drosophila* homolog of microtubule-associated protein 1B, which positively regulates microtubule stability. We previously showed that Futsch levels are increased (approximately 2-fold) in the *dfmr1* mutant brain (14). Note that the molecular mass of Futsch is >500 kDa and therefore cannot be resolved in the 2D DIGE system used here (size limit, <150 kDa; Fig. 1). Restoration of normal Futsch levels in *dfmr1* null mutants rescues both structural and functional phenotypes in the eye and neuromuscular junction (14). These results predict that the neuronal microtubule cytoskeleton is aberrantly hyperstabilized in *dfmr1* mutants. Hyperstabilization of microtubules is known to result in the formation of supernumerary processes, excess branching, and overgrowth (54–56), paralleling the *dfmr1* mutant phenotypes observed in peripheral neuromuscular junction (14) and central mushroom body neurons (19). Consistent with this hypothesis, the proteomic analysis reported here shows that a post-translationally modified isoform of β-tubulin (Fig. 1*B* and Table I, spot 23) is significantly increased in the *dfmr1* mutant brain. It will therefore be of considerable interest to confirm the change by independent assays and identify which specific isoform of β-tubulin is altered in the *dfmr1* mutants. Taken together, these results support a model in which dFMRP regulates Futsch to control microtubule stability, and loss of dFMRP therefore leads to hyperstabilized microtubules causing overextension of neuronal processes.

dFMRP has also been implicated in the independent regulation of the actin cytoskeleton. dFMRP interacts biochemically and genetically with cytoplasmic FMRP-interacting protein/Sra-1 (50) to regulate neuronal morphogenesis in both the central and peripheral nervous system. Cytoplasmic FMRP-interacting protein/Sra-1 provides a link between dFMRP-regulated translational control of the small GTPase Rac1 (17) and Rac1-mediated actin cytoskeleton remodeling of neuronal structure (17, 50). In support of these previous studies, our DIGE analyses showed a significantly increased level of actin 5C in the *dfmr1* null mutant brain. Taken together, these data suggest that dFMRP regulates both the microtubule and actin cytoskeleton in neurons. This hypothesis derived from *Drosophila* agrees well with recent data obtained from the mouse FraX model. Mammalian FMRP mRNA targets include microtubule-associated protein 1B, the mammalian homolog of *Drosophila* Futsch (9, 10), and activity-regulated cytoskeleton-associated protein Arc/Arg3.1 (9), which modulates the actin cytoskeleton. Moreover, in *fmr1* knock-out mice, elevated microtubule-associated protein 1B leads to increased neuronal microtubule stability (10), further supporting the above model (2). Alteration of cytoskeleton dynamics/stability provides a likely explanation for defects in neuronal architecture in *dfmr1* mutants, knock-out mice, and human patients. Future work is needed to elucidate the exact requirement of

dFMRP/FMRP in cytoskeleton regulation.

Up-regulation of Dopamine and Serotonin Pathways in dfmr1 Mutants—Proteomic analyses revealed that the abundance of PTM isoforms of Punch and Henna is strikingly altered in *dfmr1* mutants, favoring the up-regulation of their enzymatic activities. Punch is the rate-limiting enzyme in the synthesis of the BH4 cofactor required for Henna activity as well as tyrosine hydroxylase, the rate-limiting enzyme in the synthesis of dopamine (Fig. 4*A*). Enzymatic assays confirmed that Punch activity is elevated nearly 2-fold in *dfmr1* null mutants compared with controls. Further neurochemical HPLC measurements showed that two major monoamines, dopamine and serotonin, are significantly increased in abundance, whereas the level of octopamine, synthesized from precursor tyrosine via a BH4-independent pathway (57), remains unchanged (data not shown). Taken together, these data strongly suggest a model in which dFMRP regulates the PTM isoforms of two rate-limiting enzymes in monoamine synthesis, directly or indirectly, to negatively control the production of the neuromodulators dopamine and serotonin. Thus, in the absence of dFMRP, this regulation is lost, and dopamine, in particular, is synthesized at an aberrantly high rate. The highly elevated density of dense core vesicles in neuronal synaptic terminals of *dfmr1* mutants indicates that the excess neuromodulator is packaged for secretion.

The elevated activity of the monoamine pathway in *dfmr1* mutants suggests an underlying mechanism for the cognitive and behavioral abnormalities exhibited in human FraX patients and *fmr1* knock-out mice. First, a particularly prominent symptom in human FraX patients is hyperactivity, which is also one of the strongest phenotypes in animal models (12, 13). It is firmly established that dopamine regulates activity levels and locomotion behaviors; dopamine-deficient mice are severely hypoactive, whereas increasing synaptic concentration of dopamine by inhibiting dopamine transporters stimulates hyperactivity (24, 58). Second, recent pharmacological experiments have shown that amphetamine, a psychostimulant acting on dopamine transporter, administered to *fmr1* knock-out mice specifically enhances cognitive ability to discriminate novel *versus* familiar objects, indicating an involvement of dopamine in the cognitive defects of the mutant mice (59). Amphetamine has also been used in FraX patients to help control attention, impulsivity, and hyperactivity (60). Third, the level of melatonin is elevated in FraX patients (61). Melatonin is made in the pinealocytes of the pineal gland from serotonin in a two-step rate-limiting process, suggesting a correlation with increased levels of the precursor serotonin. Finally, turnover of dopamine and serotonin is altered in *fmr1* knock-out mice in a brain region-specific manner (51). As in *Drosophila*, the 3,4-dihydroxyphenylacetic acid level was elevated in mutant mice, although dopamine was not, resulting in an increased 3,4-dihydroxyphenylacetic acid/dopamine ratio in the mouse.

Taken together with the *Drosophila* studies shown here, these lines of evidence from mammalian studies suggest a model in which the levels of dopamine and serotonin are altered in FraX patients and knock-out mice brain, leading to clinical, cognitive, and behavioral symptoms. This model indicates that intervention to reduce dopamine/serotonin production or interfere with their biological actions should prove efficacious in the treatment of FraX symptoms. Future work will be directed at uncovering monoamine-dependent pathways to further understand the significance of this misregulated pathway on neuronal and behavioral phenotypes.

Acknowledgments—We thank Raymond Johnson from the Vanderbilt Neurochemistry Core Laboratory for help with the HPLC assays of biogenic amines and amino acids, Janna Brown for expert assistance with the enzymatic assays of Punch, and Salisha Hill for 2D DIGE analyses. We thank Heinrich Matthies of the Broadie Laboratory for insightful discussions and comments on the manuscript.

* This work was supported in part by National Institutes of Health Grants GM62879 (to J. O.) and HD40654 (to K. B.). The costs of publication of this article were defrayed in part by the payment of page charges. This article must therefore be hereby marked "*advertisement*" in accordance with 18 U.S.C. Section 1734 solely to indicate this fact.

§ Supported by postdoctoral fellowships from the FRAXA Research Foundation and the Vanderbilt Kennedy Center for Research on Human Development. Present address: Inst. of Genetics and Developmental Biology, the Chinese Academy of Sciences, Beijing 100080, China.

** To whom correspondence should be addressed: Dept. of Biological Science, Kennedy Center for Research on Human Development, Vanderbilt University, 6270A MRB III, 465 21st Ave. South, Nashville, TN 37232. Tel.: 615-936-3937 (office), or -3935, -3936, and -6761 (laboratory); Fax: 615-936-0129 (office) or 615-343-6707 (department), E-mail: kendal.broadie@vanderbilt.edu.

REFERENCES

1. Hagerman, R. J. (1996). in *Fragile X Syndrome, Diagnoses, Treatment and Research* (Hagerman, R. J., and Cronister, A., eds) pp. 3–87, The Johns Hopkins University Press, Baltimore, MD
2. Zhang, Y. Q., and Broadie, K. (2005) Fathoming fragile X in fruitflies. *Trends Genet.* **21,** 37–45
3. Jin, P., and Warren, S. T. (2003) New insights into fragile X syndrome: from molecules to neurobehaviors. *Trends Biochem. Sci.* **28,** 152–158
4. Zalfa, F., and Bagni, C (2004) Molecular insights into mental retardation: multiple functions for the fragile X mental retardation protein? *Curr. Issues Mol. Biol.* **6,** 73–88
5. Brown, V., Jin, P., Ceman, S., Darnell, J. C., O'Donnell, W. T., Tenenbaum, S. A., Jin, X., Feng, Y., Wilkinson, K. D., Keene, J. D., Darnell, R. B., and Warren, S. T. (2001) Microarray identification of FMRP-associated brain mRNAs and altered mRNA translational profiles in fragile X syndrome. *Cell* **107,** 477–487
6. Darnell, J. C., Jensen, K. B., Jin, P., Brown, V., Warren, S. T., and Darnell, R. B. (2001) Fragile X mental retardation protein targets G quartet mRNAs important for neuronal function. *Cell* **107,** 489–499
7. Miyashiro, K. Y., Beckel-Mitchener, A., Purk, T. P., Becker, K. G., Barret, T., Liu, L., Carbonetto, S., Weiler, I. J., Greenough, W. T., and Eberwine, J. (2003) RNA cargoes associating with FMRP reveal deficits in cellular functioning in Fmr1 null mice. *Neuron* **37,** 417–431
8. Chen, L., Yun, S. W., Seto, J., Liu, W., and Toth, M. (2003) The fragile X mental retardation protein binds and regulates a novel class of mRNAs containing U rich target sequences. *Neuroscience* **120,** 1005–1017
9. Zalfa, F., Giorgi, M., Primerano, B., Moro, A., Di Penta, A., Reis, S., Oostra,

B., and Bagni, C. (2003) The fragile X syndrome protein FMRP associates with BC1 RNA and regulates the translation of specific mRNAs at synapses. *Cell* **112,** 317–327
10. Lu, R., Wang, H., Liang, Z., Ku, L., O'Donnell W, T., Li, W., Warren, S. T., and Feng, Y. (2004) The fragile X protein controls microtubule-associated protein 1B translation and microtubule stability in brain neuron development. *Proc. Natl. Acad. Sci. U. S. A.* **101,** 15201–15206
11. Bakker, C. E., Verheij, C. E., Willemsen, R., van der Helm, R., Oerlemans, F., Vermeij, M., Bygrave, A., Hoogeveen, A. T., Oostra, B. A., Reyniers, E., De Boulle, K., D'Hooge, R., Cras, P., van Velzen, D., Nagels, G., Martin, J.-J., De Deyn, P., Darby, J. K., and Willems, P. J. (1994) Fmr1 knockout mice: a model to study fragile X mental retardation. *Cell* **78,** 23–33
12. O'Donnell, W. T., and Warren, S. T. (2002) A decade of molecular studies of fragile X syndrome. *Annu. Rev. Neurosci.* **25,** 315–338
13. Kooy, R. F. (2003) Of mice and the fragile X syndrome. *Trends Genet.* **19,** 148–154
14. Zhang, Y. Q., Bailey, A. M., Matthies, H. J., Renden, R. B., Smith, M. A., Speese, S. D., Rubin, G. M., and Broadie, K. (2001) *Drosophila* fragile X-related gene regulates the MAP1B homolog Futsch to control synaptic structure and function. *Cell* **107,** 591–603
15. Dockendorff, T. C., Su, H. S., McBride, S. M., Yang, Z., Choi, C. H., Siwicki, K. K., Sehgal, A., and Jongens, T. A. (2002) *Drosophila* lacking dfmr1 activity show defects in circadian output and fail to maintain courtship interest. *Neuron* **34,** 973–984
16. Morales, J., Hiesinger, P. R., Schroeder, A. J., Kume, K., Verstreken, P., Jackson, F. R., Nelson, D. L., and Hassan, B. A. (2002) *Drosophila* fragile X protein, DFXR, regulates neuronal morphology and function in the brain. *Neuron* **34,** 961–972
17. Lee, A., Li, W., Xu, K., Bogert, B. A., Su, K., and Gao, F. B. (2003) Control of dendritic development by the *Drosophila* fragile X-related gene involves the small GTPase Rac1. *Development* **130,** 5543–5552
18. Michel, C. I., Kraft, R., and Restifo, L. L. (2004) Defective neuronal development in the mushroom bodies of *Drosophila* fragile X mental retardation 1 mutants. *J. Neurosci.* **24,** 5798–5809
19. Pan, L., Zhang, Y. Q., Woodruff, E., and Broadie, K. (2004) The *Drosophila* fragile X gene negatively regulates neuronal elaboration and synaptic differentiation. *Curr. Biol.* **14,** 1863–1870
20. Wan, L., Dockendorff, T. C., Jongens, T. A., and Dreyfuss, G (2000) Characterization of dFMR1, a *Drosophila melanogaster* homolog of the fragile X mental retardation protein. *Mol. Cell. Biol.* **20,** 8536–8547
21. Siomi, M. C., Higashijima, K., Ishizuka, A., and Siomi, H. (2002) Casein kinase II phosphorylates the fragile X mental retardation protein and modulates its biological properties. *Mol. Cell. Biol.* **22,** 8438–8447
22. Jin, P., Zarnescu, D. C., Ceman, S., Nakamoto, M., Mowrey, J., Jongens, T. A., Nelson, D. L., Moses, K., and Warren, S. T. (2004) Biochemical and genetic interaction between the fragile X mental retardation protein and the microRNA pathway. *Nat. Neurosci.* **7,** 113–117
23. Tempel, B. L., Livingstone, M. S., and Quinn, W. G. (1984) Mutations in the dopa decarboxylase gene affect learning in *Drosophila*. *Proc. Natl. Acad. Sci. U. S. A.* **81,** 3577–3581
24. Zhou, Q. Y., and Palmiter, R. D. (1995) Dopamine-deficient mice are severely hypoactive, adipsic, and aphagic. *Cell* **83,** 1197–1209
25. Giros, B., Jaber, M., Jones, S. R., Wightman, R. M., and Caron, M. G. (1996) Hyperlocomotion and indifference to cocaine and amphetamine in mice lacking the dopamine transporter. *Nature* **379,** 606–612
26. Jones, S. R., Gainetdinov, R. R., Jaber, M., Giros, B., Wightman, R. M., and Caron, M. G. (1998) Profound neuronal plasticity in response to inactivation of the dopamine transporter. *Proc. Natl. Acad. Sci. U. S. A.* **95,** 4029–4034
27. McLean, J. R., Krishnakumar, S., and O'Donnell, J. M. (1993) Multiple mRNAs from the Punch locus of *Drosophila melanogaster* encode isoforms of GTP cyclohydrolase I with distinct N-terminal domains. *J. Biol. Chem.* **268,** 27191–27197
28. Ichinose, H., Ohye, T., Matsuda, Y., Hori, T., Blau, N., Burlina, A., Rouse, B., Matalon, R., Fujita, K., and Nagatsu, T. (1995) Characterization of mouse and human GTP cyclohydrolase I genes. Mutations in patients with GTP cyclohydrolase I deficiency. *J. Biol. Chem.* **270,** 10062–10071
29. Neckameyer, W. S., and White, K. (1992) A single locus encodes both phenylalanine hydroxylase and tryptophan hydroxylase activities in *Drosophila*. *J. Biol. Chem.* **267,** 4199–4206
30. Wretborn, M., Humble, E., Ragnarsson, U., and Engstrom, L. (1980) Amino acid sequence at the phosphorylated site of rat liver phenylalanine hydroxylase and phosphorylation of a corresponding synthetic peptide. *Biochem. Biophys. Res. Commun.* **93,** 403–408
31. Garber, S. L., and Makman, M. H. (1987) Regulation of tryptophan hydroxylase activity by a cyclic AMP-dependent mechanism in rat striatum. *Brain Res.* **427,** 1–10
32. Makita, Y., Okuno, S., and Fujisawa, H. (1990) Involvement of activator protein in the activation of tryptophan hydroxylase by cAMP-dependent protein kinase. *FEBS Lett.* **268,** 185–188
33. Hesslinger, C., Kremmer, E., Hultner, L., Ueffing, M., and Ziegler, I. (1998) Phosphorylation of GTP cyclohydrolase I and modulation of its activity in rodent mast cells. GTP cyclohydrolase I hyperphosphorylation is coupled to high affinity IgE receptor signaling and involves protein kinase C. *J. Biol. Chem.* **273,** 21616–21622
34. Coleman, C. M., and Neckameyer, W. S. (2004) Substrate regulation of serotonin and dopamine synthesis in *Drosophila*. *Invert. Neurosci.* **5,** 85–96
35. Zhang, Y. Q., Matthies, H. J., Mancuso, J., Andrews, H. K., Woodruff, E., III, Friedman, D., and Broadie, K. (2004) The *Drosophila* fragile X-related gene regulates axoneme differentiation during spermatogenesis. *Dev. Biol.* **270,** 290–307
36. Friedman, D. B., Hill, S., Keller, J. W., Merchant, N. B., Levy, S. E., Coffey, R. J., and Caprioli, R. M. (2004) Proteome analysis of human colon cancer by two-dimensional difference gel electrophoresis and mass spectrometry. *Proteomics* **4,** 793–811
37. Alban, A., David, S. O., Bjorkesten, L., Andersson, C., Sloge, E., Lewis, S., and Currie, I. (2003) A novel experimental design for comparative two-dimensional gel analysis: two-dimensional difference gel electrophoresis incorporating a pooled internal standard. *Proteomics* **3,** 36–44
38. Gutlich, M., Witter, K., Bourdais, J., Veron, M., Rodl, W., and Ziegler, I. (1996). Control of 6-(D-threo-1′,2′-dihydroxypropyl)pterin (dictyopterin) synthesis during aggregation of Dictyostelium discoideum. Involvement of the G-protein-linked signalling pathway in the regulation of GTP cyclohydrolase I activity. *Biochem. J.* **314,** 95–101
39. Krishnakumar, S., Burton, D., Rasco, J., Chen, X., and O'Donnell, J. (2000) Functional interactions between GTP cyclohydrolase I and tyrosine hydroxylase in *Drosophila*. *J. Neurogenet.* **14,** 1–23
40. Cohen, S. A., and Michaud, D. P. (1993) Synthesis of a fluorescent derivatizing reagent, 6-aminoquinolyl-N-hydroxysuccinimidyl carbamate, and its application for the analysis of hydrolysate amino acids via high-performance liquid chromatography. *Anal. Biochem.* **211,** 279–287
41. Cransac, H., Cottet-Emard, J. M., Pequignot, J. M., and Peyrin, L. (1996) Monoamines (norepinephrine, dopamine, serotonin) in the rat medial vestibular nucleus: endogenous levels and turnover. *J. Neural Transm.* **103,** 391–401
42. Lindsey, J. W., Jung, A. E., Narayanan, T. K., and Ritchie, G. D. (1998) Acute effects of a bicyclophosphate neuroconvulsant on monoamine neurotransmitter and metabolite levels in the rat brain. *J. Toxicol. Environ. Health A* **54,** 421–429
43. Broadie, K. S., and Richmond, J. E. (2002) Establishing and sculpting the synapse in *Drosophila* and C. elegans. *Curr. Opin. Neurobiol.* **12,** 491–498
44. Jin, P., and Warren, S. T. (2000) Understanding the molecular basis of fragile X syndrome. *Hum. Mol. Genet.* **9,** 901–908
45. Greenough, W. T., Klintsova, A. Y., Irwin, S. A., Galvez, R., Bates, K. E., and Weiler, I. J. (2001) Synaptic regulation of protein synthesis and the fragile X protein. *Proc. Natl. Acad. Sci. U. S. A.* **98,** 7101–7106
46. Li, Z., Zhang, Y., Ku, L., Wilkinson, K. D., Warren, S. T., and Feng, Y. (2001) The fragile X mental retardation protein inhibits translation via interacting with mRNA. *Nucleic Acids Res.* **29,** 2276–2283
47. Schaeffer, C., Bardoni, B., Mandel, J. L., Ehresmann, B., Ehresmann, C., and Moine, H. (2001) The fragile X mental retardation protein binds specifically to its mRNA via a purine quartet motif. *EMBO J.* **20,** 4803–4813
48. Qin, M., Kang, J., and Smith, C. B. (2002) Increased rates of cerebral glucose metabolism in a mouse model of fragile X mental retardation. *Proc. Natl. Acad. Sci. U. S. A.* **99,** 15758–15763
49. Feder, M. E., and Hofmann, G. E. (1999) Heat-shock proteins, molecular chaperones, and the stress response: evolutionary and ecological physiology. *Annu. Rev. Physiol.* **61,** 243–282
50. Schenck, A., Bardoni, B., Langmann, C., Harden, N., Mandel, J. L., and

Giangrande, A. (2003) CYFIP/Sra-1 controls neuronal connectivity in *Drosophila* and links the Rac1 GTPase pathway to the fragile X protein. *Neuron* **38,** 887–898
51. Gruss, M., and Braun, K. (2004) Age- and region-specific imbalances of basal amino acids and monoamine metabolism in limbic regions of female Fmr1 knock-out mice. *Neurochem. Int.* **45,** 81–88
52. Vie, A., Cigna, M., Toci, R., and Birman, S (1999) Differential regulation of *Drosophila* tyrosine hydroxylase isoforms by dopamine binding and cAMP-dependent phosphorylation. *J. Biol. Chem.* **274,** 16788–16795
53. Chu, R., Lim, H., Brumfield, L., Liu, H., Herring, C., Ulintz, P., Reddy, J. K., and Davison, M. (2004) Protein profiling of mouse livers with peroxisome proliferator-activated receptor alpha activation. *Mol. Cell. Biol.* **24,** 6288–6297
54. Dehmelt, L., Smart, F. M., Ozer, R. S., and Halpain, S (2003) The role of microtubule-associated protein 2c in the reorganization of microtubules and lamellipodia during neurite initiation. *J. Neurosci.* **23,** 9479–9490
55. Buck, K. B., and Zheng, J. Q. (2002) Growth cone turning induced by direct local modification of microtubule dynamics. *J. Neurosci.* **22,** 9358–9367
56. Gordon-Weeks, P. R., and Fischer, I. (2000) MAP1B expression and microtubule stability in growing and regenerating axons. *Microsc. Res. Tech.* **48,** 63–74
57. Monastirioti, M. (1999) Biogenic amine systems in the fruit fly *Drosophila melanogaster*. *Microsc. Res. Tech.* **45,** 106–121
58. Woolverton, W. L., and Johnson, K. M. (1992) Neurobiology of cocaine abuse. *Trends Pharmacol. Sci.* **13,** 193–200
59. Ventura, R., Pascucci, T., Catania, M. V., Musumeci, S. A., and Puglisi-Allegra, S. (2004) Object recognition impairment in Fmr1 knockout mice is reversed by amphetamine: involvement of dopamine in the medial prefrontal cortex. *Behav. Pharmacol.* **15,** 433–442
60. Hagerman, R. J. (1996) in *Fragile X Syndrome, Diagnoses, Treatment and Research* (Hagerman, R. J., and Cronister, A., eds) pp. 283–331, The Johns Hopkins University Press, Baltimore, MD
61. Gould, E. L., Loesch, D. Z., Martin, M. J., Hagerman, R. J., Armstrong, S. M., and Huggins, R. M. (2000) Melatonin profiles and sleep characteristics in boys with fragile X syndrome: a preliminary study. *Am. J. Med. Genet.* **95,** 307–315